Analytical theory of NEXAFS from diatomic molecules

V. L. Shneerson and W. T. Tysoe
Department of Chemistry and Laboratory for Surface Studies, University of Wisconsin–Milwaukee, P.O. Box 413, Milwaukee, Wisconsin 53201

D. K. Saldin
Department of Physics and Laboratory for Surface Studies, University of Wisconsin–Milwaukee, P.O. Box 413, Milwaukee, Wisconsin 53201

(Received 12 September 1995; revised manuscript received 18 December 1995)

Analytical expressions are derived for both the π^* and σ^* resonances in near-edge x-ray-absorption fine-structure (NEXAFS) spectra from diatomic molecules. A simple criterion is formulated for extracting structural parameters (e.g., the bond lengths) of such molecules from NEXAFS spectra. A universal curve for the positions of resonances is derived from our analytical expressions. The predictions are confirmed by comparisons with computer simulations of NEXAFS spectra for gas-phase N_2 and O_2 molecules.

I. INTRODUCTION

The fine structure found beyond the onset of an absorption edge on an x-ray-absorption spectrum (XAS) from a sample of condensed matter arises from the effects on the quantum-mechanical transition matrix elements, due to the backscattering from surrounding atoms of ejected atomic core electrons. As such, an XAS is a rich repository of information on the crystallographic and electronic structure in the vicinity of the atom absorbing the x-ray photon. The absorption fine structures are conventionally divided into two distinct regions characterized by their proximities to the absorption edge. The structure found beyond about 50 eV from an absorption edge is termed the extended x-ray-absorption fine structure (EXAFS), while that closer to the absorption edge is known as the near-edge x-ray-absorption fine structure (NEXAFS).

This division is not purely arbitrary. Due to its higher energy, the backscattering of an electrons giving rise to EXAFS is well described by the single scattering, or kinematic theory of diffraction. As a result of this simplification, the extraction of structural information from EXAFS spectra is relatively straightforward, and achievable by the standard mathematical device of Fourier transformation.[1–3] Due to the lower energy of an ejected electron giving rise to NEXAFS, however, a kinematic theory is not adequate to account for the form of the latter spectral modulations. Instead, a proper understanding of NEXAFS spectra is to be found only in the context of the much more complicated multiple-scattering theory.[4–7]

That the effort is worthwhile is evidenced by the wealth of structural information already provided by NEXAFS about surfaces, bulk materials, and even of isolated molecules.[8] In principle, near-edge spectra can yield information on the coordination geometry, molecular orientation, and on the density and symmetry of unoccupied valence electron states. It is also particularly useful for the determination of the structure of surface species, since it can easily be made surface sensitive by detecting either the total secondary electron yield or even the Auger decay rate of the core hole that is created by the resonant excitation from that core level.

The usual strategy for analyzing experimental NEXAFS spectra is to begin by proposing a set of trial atomic structures in the vicinity of the absorbing atoms. Using one of the established multiple-scattering computer codes, the expected spectra from each of these model structures is calculated, in order to find a best fit to the measured spectra. This is often a tedious and time-comsuming procedure. In addition, this process relies on one of the guessed structures being correct. Absent is the kind of direct algorithmic prescription afforded by the more analytic understanding of EXAFS.

The aim of this paper is to propose a more analytical approach to NEXAFS. As a first step in this direction, we restrict our attention to diatomic gas-phase molecules. This is not quite as much of a restriction as might first be thought: there are a large number of homonuclear and heteronuclear molecules of great interest, for example, Co, N_2, and H_2. In addition, there are also a large number of ''pseudo'' heteronuclear diatomic molecules, i.e., those molecules that contain hydrogen, and so to first-order treatable as heteronuclear diatomic molecules, since the hydrogen atoms in these molecules scatter electrons only rather weakly. Examples of these include important surface species, such as adsorbed methoxy or methane thiolate groups.

In developing an analytic strategy for analyzing NEXAFS spectra, we first discuss the polarization dependence of the x-ray-absorption rate and derive the required elements of the multiple-scattering matrix τ. Next, the symmetry restrictions for a simple diatomic molecule are taken into consideration to clarify the structure of multiple-scattering reflection matrix R and free-electron propagators g. Analytical expressions for molecular π^* and σ^* resonances are then derived both with and without contributions from higher spherical harmonics. Finally, an analytical criterion for predicting the position of NEXAFS peaks is formulated and illustrated using the simple case of nitrogen (N_2) and oxygen (O_2) molecules.

II. THEORY OF X-RAY-ABSORPTION RATE

A. General theory

The x-ray-absorption rate can be calculated from the Fermi golden rule for the transition probability per unit time $W_c(\omega)$ from an initial core state of energy E_c, to final states of energy $E_c+\omega$ driven by a perturbation $\Delta(\underline{r})$ as

$$W_c(E)=2\pi|M(E)|^2\rho_f(E), \tag{1}$$

where $\rho_f(E)$ is the density of final states. In the above expression as well as the ones that follow, we use hartree atomic units, where $e=m=\hbar=1$, where e and m are the charge and mass of the electron, and $\hbar$ is Planck's constant divided by 2π. The excitation matrix element is

$$M_{nl'm',lm}=\int \Psi^*_{lm}(\mathbf{r},E)\Delta(\mathbf{r})\Phi_{nl'm'}(\mathbf{r})d\mathbf{r}, \tag{2}$$

where Ψ_{lm} and $\Phi_{nl'm'}$ are the wave functions of final and initial (core) states, respectively.

In the dipole approximation, the electromagnetic field's excitation operator is equal to

$$\Delta(\mathbf{r})=-\frac{\mathbf{Ap}+\mathbf{pA}}{2}=-\mathbf{Ap},$$

where the Coulomb gauge $\boldsymbol{\nabla}\mathbf{A}=\mathbf{0}$ of a vector potential $\mathbf{A}$ is chosen. Using the operator equivalents for the momentum operator $\mathbf{p}$,[9] and applying them within the range of the potential field $V(\mathbf{r})$,

$$\mathbf{p}=\frac{i}{E_f-E_i}\boldsymbol{\nabla}V(\mathbf{r}),$$

one can get that

$$\Delta(\mathbf{r})=-\frac{i}{\omega}\mathbf{A}\boldsymbol{\nabla}V(r), \tag{3}$$

with the x-ray photon frequency $\omega=E_f-E_i$.

Thus, for the particular case of K-edge excitation (where the initial state's momentum and magnetic quantum numbers are $l=0,\ m=0$) we can represent the matrix element (2) in the form

$$M_{00,lm}=-\frac{i}{\omega}\int \Psi^*_{lm}(\mathbf{r},E)\mathbf{A}\boldsymbol{\nabla}V(r)\Phi_{100}(\mathbf{r})d\mathbf{r}. \tag{4}$$

Inserting, here, the representation of $\Psi_{lm}=R_l(r,E)Y_{lm}(\vartheta,\phi)$ and $\boldsymbol{\nabla}V(r)=(\partial V/\partial r)\hat{r}$, we get the result

$$M_{oo,lm}=-\frac{i}{\omega}\int R_l(r,E)\frac{\partial V}{\partial r}R_{10}(r)r^2dr \times\int \mathbf{A}\hat{r}Y^*_{lm}(\hat{r})Y_{00}(\hat{r})d\Omega. \tag{5}$$

Introducing the x-ray polarization vector,

$$\hat{\epsilon}=\frac{\mathbf{A}}{|\mathbf{A}|},$$

and using the addition theorem for spherical harmonics gives

$$\mathbf{A}\hat{r}=A\hat{\epsilon}\hat{r}=A\cos(\gamma)=\frac{4\pi}{3}A\sum_{m=-1}^{1}Y^*_{lm}(\hat{\epsilon})Y_{lm}(\hat{r}).$$

Equations (3) and (4) can then be combined to yield, for the transition matrix element, the formula

$$M_{00,lm}=-\frac{4\pi i}{\omega}A\frac{1}{\sqrt{4\pi}}\int R_l(r,E)\frac{\partial V}{\partial r}R_{10}(r)r^2dr\sum_{m'=-1}^{1} \times\int Y^*_{lm'}(\hat{r})Y_{lm'}(\hat{r})d\Omega_r Y^*_{1m}(\hat{\varepsilon}). \tag{6}$$

Defining the radial part of matrix element as

$$M^{\rm rad}_{0,l}(E)=-\frac{\sqrt{4\pi i}}{\omega}A\int R_l(r,E)\frac{\partial V}{\partial r}R_{10}(r)r^2dr, \tag{7}$$

and making use of the orthonormality condition,

$$\int Y^*_{lm}(\hat{r})Y_{lm}(\hat{r})d\Omega_r=\delta_{l1}\delta_{mm},$$

results in

$$M_{00,lm}(E,\hat{\epsilon})=\delta_{l1}M_{00,1m}(E,\hat{\epsilon})=\delta_{l1}M^{\rm rad}_{01}(E)Y^*_{1m}(\hat{\varepsilon}). \tag{8}$$

According to Ref. 4, the transition probability (1) may be rewritten in the form

$$W(E)=-2k\ {\rm Im}\times\left\{\sum_{m,m=-1}^{1}M_{00,1m}(E,\hat{\varepsilon})\frac{\tau_{1m,1m'}}{\sin^2\delta_1}M^*_{00,1m'}(E,\hat{\varepsilon})\right\}, \tag{9}$$

where δ_1 is a phase shift for the spherical partial wave described by quantum numbers (l,m), and with wave number $k=\sqrt{2E}$. The scattering path operator τ (with matrix elements $\tau_{lm,l'm'}$) sums all paths that begin and end at the central atom and includes all intermediate multiple-scattering events. Thus, from Eqs. (8) and (9), this yields for the adsorption cross section:

$$W(E)=-2k|M^{\rm rad}_{01}(E)|^2\times{\rm Im}\left(\sum_{m,m'=-1}^{1}\frac{\tau_{1m,1m'}}{\sin^2\delta_1}Y_{1m}(\hat{\varepsilon})Y^*_{1m'}(\hat{\varepsilon})\right). \tag{10}$$

B. Linear molecules

This equation may be evaluated analytically for the simple case of a linear molecule. As noted above, this sample class still includes a large number of examples of chemical and physical interest. Since these molecules are characterized by either $C_{\infty v}$ or $D_{\infty h}$ point symmetry, there is no azimuthal angular dependence in the absorption cross section, so that only the $m=m'$ components of the spherical harmonics contribute to the right-hand side of Eq. (10). It may, therefore, be simplified to yield

$$W(E)=-\frac{3k}{2\pi\ \sin^2\delta_1}|M_{01}^{\mathrm{rad}}(E)|^2 \times \mathrm{Im}\{\tau_{11,11}\sin^2\theta+\tau_{10,10}\cos^2\theta\}, \qquad (11a)$$

where θ is the angle between the polarization electric-field vector $\hat{\varepsilon}$ and the z axis pointing along the internuclear axis of the absorbing molecule.

For a gas-phase molecule, it is an angularly integrated spectrum that is generally measured, since the molecule rotates freely. This case will be addressed here. It may be easily extended to the case of an oriented molecule adsorbed on a surface. Clearly, in either case, the positions of the resonances will be identical; only the details of the spectra will vary. Since we are primarily interested in the energies of the resonances, this is not a problem. Because $\langle\sin^2\theta\rangle=2\langle\cos^2\theta\rangle=\frac{2}{3}$, the observed angularly integrated spectrum is described by the expression

$$W(E)=-\frac{k}{2\pi\ \sin^2\delta_1}|M_{01}^{\mathrm{rad}}(E)|^2\mathrm{Im}\{2\tau_{11,11}+\tau_{10,10}\}. \qquad (11b)$$

In this case, the matrix element $\tau_{10,10}$ with zero angular momentum projection along the z axis represents the σ resonance, and $\tau_{11,11}$ is responsible for the π peak.

The scattering path operator τ is given[4,5,10] in terms of the elements

$$t_l^0(E)=i\ \sin\delta_l(E)\exp(i\,\delta_l(E)) \qquad (12)$$

of the atomic scattering matrix t^0 of the central atom, where δ_l is the corresponding atomic phase shift of angular momentum quantum number l, and the ''out-in'' reflection matrix $R_{lm,l'm'}(E)$ of the surrounding cluster of atoms:

$$\tau=it^0(1-Rt^0)^{-1}. \qquad (13)$$

All complications arising from calculating the τ operator are due to the inversion of multidimensional matrices. The necessity of one of these inversions is obvious just from the expression (13). Another follows from the definition of the reflection matrix:

$$R_{lm,l'm'}=\sum_{i,j}\sum_{l_1,m_1}\sum_{l_2,m_2} g^{oi}_{lm,l_1m_1}T^{ij}_{l_1m_1,l_2m_2}g^{jo}_{l_2m_2,l'm'}, \qquad (14)$$

where the two-centered free-electron propagator $g^{oi}_{lm,l'm'}$ describes the propagation of the electron in a spherical wave representation from the central atom o to atom i. The T matrix is the inverse of the real-space KKR matrix $H^{ij}=(t^{-1})^{ij}\delta_{ij}-g^{ij}$, where t is a matrix constructed from the scattering amplitudes of the atoms constituting the surrounding cluster, and g^{ij} is the propagator from atom i to atom j in the same cluster. Thus,

$$T=(t^{-1}-g)^{-1}. \qquad (15)$$

Only two components of the multiple-scattering matrix, namely, $\tau_{11,11}$ and $\tau_{10,10}$ are required for the transition rate calculation [Eq. (11)]. This is the first of the key factors allowing the development of an analytical theory for a linear molecule.

A second important simplification may be made in the case of a diatomic molecule. In this case, the cluster of atoms surrounding the absorbing atom contains just the single other atom of the molecule, and hence the intrashell propagators g^{ij} do not exist, since $i=j=1$, and therefore,

$$T^{ij}_{lm,l'm'}(E)=\delta_{i1}\delta_{j1}\delta_{mm'}\delta_{ll'}t_l(E). \qquad (16)$$

Substitution of Eq. (16) into Eq. (14) yields

$$R_{lm,l'm'}(E)=\sum_{l_1m_1} g^{01}_{lm,l_1m_1}(E)t_{l_1}(E)g^{10}_{l_1m_1,l'm'}(E). \qquad (17)$$

Finally, a third key ingredient, which enables the formulation an analytical expression for the scattering-path operator, are the restrictions imposed on the reflection matrix, R, and g propagators by the linear geometry of the molecule. This effect will be discussed in greater detail in the following section.

1. Diagonality of the matrices in the subspace of magnetic quantum numbers

The basis functions Y_{lm} in the spherical wave representation referred to the origin of coordinates at the central atom are eigenfunctions of an operator of rotation $\hat{C}_n$ through an angle $\varphi=2\pi/n$:

$$\hat{C}_nY_{lm}=\exp(2\pi im/n)Y_{lm}.$$

This rotation initiates a transformation of the reflection matrix:

$$\hat{C}_nR_{lm,l'm'}=\exp[2\pi i(m-m')/n]R_{lm,l'm'}. \qquad (18)$$

That is because, from Eq. (17), the transformation properties of R matrix, with respect to the first pair of indices (l,m), are the same as for the propagator's matrix $g_{lm,\ldots}$, which transforms in accordance with Eqs. (24) and (26) below, like the function Y_{lm}. As for the second pair of indices, the transformation properties are determined by

$$R_{\ldots,l'm'}\sim g_{\ldots,l'm'}\sim B(\ldots,l'm',\ldots)\sim Y_{l'-m'}.$$

For a molecule with an n-fold symmetry, the reflection matrix should remain unchanged under the transformation in Eq. (18). Therefore, the possible range of values m-m' is restricted by the condition

$$m-m'=0,\pm n,\pm 2n,\pm 3n,\ldots. \qquad (19)$$

The symmetry of point group for a linear molecule can either be $D_{\infty h}$ (e.g., CO_2, N_2) or $C_{\infty v}$ (e.g., CO). As $n\to\infty$, and for finite values of m and m', the condition expressed in Eq. (19) may be satisfied only for $m-m'=0$. Thus, the reflection matrix is subdiagonal, with respect to the magnetic quantum numbers m:

$$R_{lm,l'm'}=\delta_{mm'}R^{(m)}_{ll'}. \qquad (20)$$

It is useful to order the components of the reflection matrix, by introducing a collective index N, which has a one-to-one correspondence to the pair of quantum numbers (l,m), according to the rule

$$N=l(l+1)+m+1 \tag{21}$$

[where the states follow the order (0,0); (1,−1); (1,0); (2,−2); (2,−1); etc.]. In this folded-down notation, the reflection matrix for linear molecules has the structure

$$\begin{pmatrix} R_{11} & 0 & R_{13} & 0 & . \\ 0 & R_{22} & 0 & 0 & . \\ R_{13} & 0 & R_{33} & 0 & . \\ 0 & 0 & 0 & R_{44} & . \\ . & . & . & . & . \end{pmatrix}. \tag{22}$$

To clarify the matrix structure of free-electron propagators g, we need the explicit form of these functions:[4]

$$g^{ij}_{lm,l'm'}(k\mathbf{r}_{ij})=4\pi\sum_{l''m''} i^{l-l'-l''}(-1)^{m'+m''}h^{(1)}_{l''}(kr_{ij}) \times Y_{l'',-m''}(\hat{\mathbf{r}}_{ij})B(lm,l'm',l''m''), \tag{23}$$

where $h^{(1)}_l$ is the Hankel function, $k(=\sqrt{2E})$ the wave number of the propagating electron, $\mathbf{r}_{ij}$ is the position vector joining the ith and jth atoms, and

$$B(lm,l'm',l''m'')=\int Y_{lm}Y_{l''m''}Y_{l',-m'}d\Omega, \tag{24}$$

Taking the unit vector $\hat{\mathbf{r}}_{ij}$ in the direction of the chemical bond of the linear molecule to be the z axis, it may be expressed in the spherical coordinates (r,θ,φ) as $\hat{\mathbf{r}}_{ij}=(1,0,0)$. Because of this the spherical harmonic $Y_{l'',-m''}(\hat{\mathbf{r}}_{ij})$ in Eq. (23) is equal to zero unless $m''=0$,

$$Y_{l'',-m''}(0,0)=\delta_{m''0}\left(\frac{2l''+1}{4\pi}\right)^{\frac{1}{2}} \tag{25}$$

Therefore, the g matrix (23) is diagonal, with respect to magnetic quantum numbers,

$$g^{ij}_{lm,l'm'}=\delta_{mm'}\sqrt{4\pi}\sum_{l''}\sqrt{2l''+1}(-1)^m i^{l-l'-l''}h^{(1)}_{l''}(kr_{ij}) \times B(lm,l'm,l''0). \tag{26}$$

Of course, this diagonality arises from the same symmetry imposed restrictions as the diagonality of the reflection matrix (20). These expressions will be used to calculated the positions of the resonances corresponding to the maxima in the NEXAFS spectrum.

2. Diatomic molecules: Explicit form for molecular absorption peaks

For the small kinetic energies encountered in the NEXAFS region ($E_k<50$ eV), the atomic scattering amplitudes, t^0_l, [Eq. (16)], of higher angular momenta would be expected to be small.[11] This implies that only the first two partial (s and p) waves need to be included in the calculation to yield relatively accurate results. The straightforward generalization to higher harmonics is included in an Appendix.

The matrix X, where

$$X=(1-Rt^0)^{-1}, \tag{27}$$

is introduced, which allows us to represent the τ matrix (13) as

$$\tau=it^0X. \tag{28}$$

Equation (27) may then be written as

$$\begin{pmatrix} 1-R_{11}t^0_s & 0 & R_{13}t^0_p & 0 \\ 0 & 1-R_{22}t^0_p & 0 & 0 \\ R_{13}t^0_s & 0 & 1-R_{33}t^0_p & 0 \\ 0 & 0 & 0 & 1-R_{44}t^0_p \end{pmatrix} \times\begin{pmatrix} X_{11} & X_{12} & X_{13} & X_{14} \\ X_{21} & X_{22} & X_{23} & X_{24} \\ X_{31} & X_{32} & X_{33} & X_{34} \\ X_{41} & X_{42} & X_{43} & X_{44} \end{pmatrix}=\begin{pmatrix} 1 & 0 & 0 & 0 \\ 0 & 1 & 0 & 0 \\ 0 & 0 & 1 & 0 \\ 0 & 0 & 0 & 1 \end{pmatrix}, \tag{29}$$

where the reflection matrix (22) has been used. For the evaluation of the transition rate $W(E)$, see Eq. (11b), we need to find only two elements of the X matrix, namely:

$$X_{33}=\frac{\tau_{10,10}}{it^0_p}, \quad X_{44}=\frac{\tau_{11,11}}{it^0_p}. \tag{30}$$

The first one describes the excitation into a state with symmetrical charge distribution around the z axis (an $m=0$ or σ state), while the second expression corresponding to $m=1$ results in excitation into a π state.

The variable X_{44} is not coupled to other elements of the X matrix and satisfies the equation

$$(1-R_{44}t^0_p)X_{44}=1. \tag{31}$$

To find the element X_{33}, it is necessary to solve the simultaneous equations:

$$\begin{pmatrix} 1-R_{11}t^0_s & -R_{13}t^0_p \\ -R_{13}t^0_s & 1-R_{33}t^0_p \end{pmatrix}\begin{pmatrix} X_{13} \\ X_{33} \end{pmatrix}=\begin{pmatrix} 0 \\ 1 \end{pmatrix}, \tag{32}$$

which finally yields

$$\tau_{11,11}\equiv\tau_{44}=\tau_{22}=\frac{it^0_p}{1-R_{44}t^0_p}, \tag{33}$$

$$\tau_{10,10}\equiv\tau_{33}=\frac{it^0_p}{1-R_{33}t^0_p-\dfrac{(R_{13})^2t^0_st^0_p}{1-R_{11}t^0_s}}.$$

A more general form of the matrix elements τ_{22} and τ_{33}, including higher angular momentum terms up to $1=2$, are included as Appendix A.

3. s- and p-wave scattering: Analytic form for reflection matrix elements

Expressions for the components of the reflection matrix are given in Appendix B. Consistent with the approach used to derive Eq. (33), only s- and p-scattering events are taken below into account. In terms of the dimensionless parameter $x(=k\rho)$, where ρ is the internuclear separation,

$$R_{44}=\left(\frac{3h_1^{(1)}(x)}{x}\right)^2 t_p, \tag{34}$$

$$R_{33}=(\sqrt{3}h_1^{(1)}(x))^2 t_s+\left(3\frac{dh_1^{(1)}(x)}{dx}\right)^2 t_p, \tag{35}$$

$$R_{13}=\sqrt{3}h_0^{(1)}(x)h_1^{(1)}(x)t_s-3\sqrt{3}h_1^{(1)}(x)\frac{dh_1^{(1)}(x)}{dx}t_p, \tag{36}$$

$$R_{11}=(h_0^{(1)}(x))^2 t_s+3(h_1^{(1)}(x))^2 t_p, \tag{37}$$

We may represent the expressions (33) for the τ-matrix elements in the form

$$\tau_{11,11}=\frac{it_p^0}{1-\Sigma_\pi},$$

$$\tau_{10,10}=\frac{it_p^0}{1-\Sigma_\sigma}, \tag{38}$$

where the Σ functions are

$$\Sigma_\pi=R_{44}t_p^0=\left(\frac{3h_1^{(1)}(x)}{x}\right)^2 t_p t_p^0,$$

$$\Sigma_\sigma=R_{33}t_p^0+\frac{(R_{13})^2 t_s^0 t_p^0}{1-R_{11}t_s^0}. \tag{39}$$

Together with Eqs. (11a) or (11b), these equations constitute analytical expressions for NEXAFS spectra from a diatomic molecule. For practical purposes, often the detailed shape of the entire spectrum may not be required, rather just the positions of the maxima of any resonances. An even simpler criterion for these will be derived in the next section.

III. CRITERION FOR THE POSITIONS OF RESONANCES

The representation of the τ matrix elements in the form of Eq. (38) is useful to establish the conditions for the resonances in the NEXAFS spectrum. One should expect that, in the vicinity of the resonance, the corresponding matrix element (either $\tau_{11,11}$ for π resonance or $\tau_{10,10}$ for σ resonance) will be large, so that it leads to a peak in the absorption coefficient (11b), as a function of energy. According to Eq. (38), this would follow if the real and imaginary parts of both $1-\Sigma_\pi$ or $1-\Sigma_\sigma$ are small. Neglecting the rather slow dependence of the atomic phase shifts $\delta(k)$ on k, we may write

$$f(x)=\mathrm{Re}(1-\Sigma), \quad \varphi(x)=\mathrm{Im}(1-\Sigma)=-\mathrm{Im}(\Sigma). \tag{40}$$

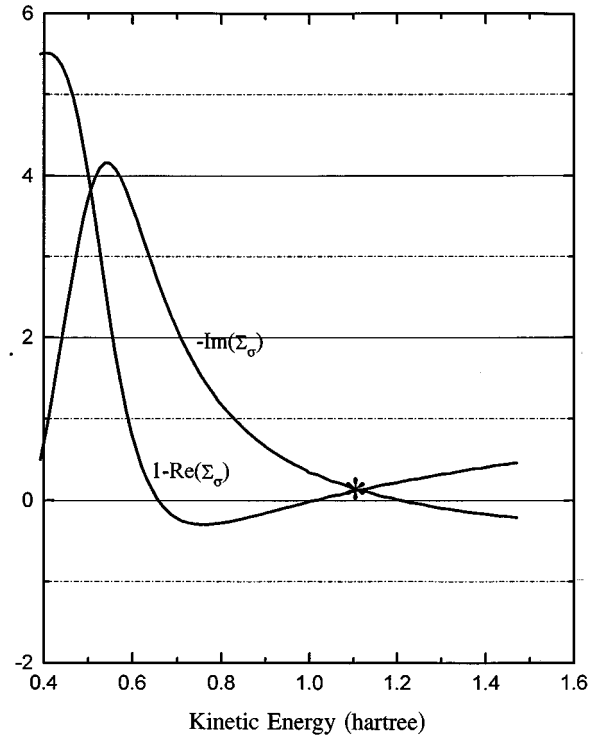

FIG. 1. Real and imaginary parts of the function $1-\Sigma_\sigma$, for the case of gas-phase N_2 molecule. Note the coincidence between the intersection point [i.e., the root of Eq. (41)] and the position of the σ resonance, indicated by the asterisk. Only the root corresponding to small values of $|1-\Sigma_\sigma|\ll 1$ indicates the position of a resonance peak (the intersection at small energies occurs at $|1-\Sigma_\sigma|\approx 4$ and does not correspond to a resonance).

An estimate of the resonance positions may be obtained by setting

$$f(x)=\varphi(x), \tag{41}$$

where they are both small. The latter requirement may be stated mathematically as $-H_2<f,\varphi<H_1$, with $H_1\sim H_2\ll 1$. Since there is no reason to expect that the derivatives of these functions $df/dx\sim d\varphi/dx\sim\nu$ will be small in the same region, the range, Δx, of the x axis, over which both f and φ would be expected to be small, may be estimated by

$$\Delta x\sim\frac{H}{df/dx}\sim\frac{H}{d\varphi/dx}\sim\frac{H}{\nu}\ll 1. \tag{42}$$

Thus, the error in determining a resonance peak position from the intersection of the functions f and φ is Δx, which is in turn $\ll 1$. This is illustrated in Fig. 1, where the real and imaginary parts of the function $1-\Sigma$ are plotted for the case of the σ resonance (the position of which is indicated by the asterisk) of gas-phase N_2 molecule. Note that the intersection point that occurs in the region of the small energies does not lead to a resonance, since the value of $1-\Sigma$ is not sufficiently small.

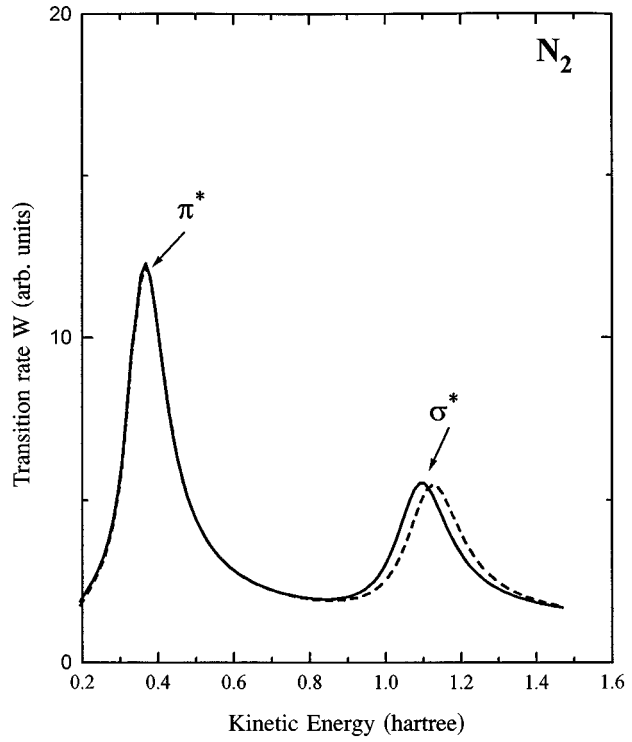

FIG. 2. Calculated NEXAFS spectra (arb. units) of gas-phase nitrogen N_2: solid line—exact computer simulation; dashed line—calculation using the analytical expressions (33)–(37) with only two (s and p) spherical harmonics. When d spherical harmonics are added, the analytical spectra are indistinguishable from the result of the exact computer simulation (solid line).

IV. COMPARISON OF ANALYTICAL THEORY WITH COMPUTER SIMULATIONS

To illustrate the validity of the analytical expressions for the τ-matrix elements and also for the criterion (41) for the position of a resonance, we have calculated the NEXAFS spectrum for the nitrogen and oxygen gas-phase molecules. For these calculations, we have evaluated the atomic scattering amplitudes, using the *constant chemical-potential–local-density approximation* (CCP-LDA) method proposed earlier,[12] and which has been successfully applied[13] to the calculation of the NEXAFS spectra of a number of small gas-phase molecules.

The resulting calculated NEXAFS spectrum of N_2 is shown in Fig. 2. The solid line represents the result of an exact computer simulation by means of the computer code of Vvedensky, Saldin, and Pendry.[5] The positions of the peaks are in good agreement with the experimental measurements,[14] even without corrections, due to excited-state core-hole effects, implying that final-state screening effects are not significant for such gas-phase diatomic molecules. As a test, we have calculated the N_2 NEXAFS in the so-called $Z+1$ approximation, where the scattering potential of the excited atom is replaced by that of the next higher element in the Periodic Table (O in this case). We found a difference only in the absolute energies of the π^* and σ^* resonances, and not in their separation. As for the absolute energies of, e.g., the $1s$ to π^* transition, we found that our frozen-orbital approximation (402 eV) yielded a much better agreement with experiment (401 eV) (Ref. 15), than the $Z+1$ approximation (407 eV).

The π^* resonance of a diatomic molecule, such as O_2 or N_2 is, of course, determined by the molecular-orbital splitting of the atomic p orbitals oriented perpendicular to the interatomic axis. This splitting gives rise to an occupied molecular π orbital, downshifted relative to the atomic p orbital, and an upshifted unoccupied π^* resonance, which appears as the first major peak of a K-edge NEXAFS spectrum of such a molecule. This picture is confirmed for N_2 by Fig. 2, which indicates a π^* resonance at an electron kinetic energy of 0.38 hartrees, while the corresponding kinetic energy of a purely *atomic* $1s$ to $2p$ transition was found to be 0.18 hartrees (from the energy of the resonance of the atomic p phase shift).

The dashed line in Fig. 2 represents the spectrum calculated from the analytical expressions (33)–(37) and those for the elements of the reflection matrix R given in Appendix B, using only two (s and p) spherical harmonics. The small shift in the position of σ resonance, compared with the computer simulations, is caused by the increasing role of the d wave function at higher energies. If account is taken of d scattering, as well as of s and p scattering, complete coincidence is obtained between results obtained by computer simulation and by those using the analytical expressions derived in Appendix A. The correspondence between the NEXAFS peak positions and the intersection points of the real and imaginary part of the $1-\Sigma$ function is illustrated in Fig. 3, for oxygen and nitrogen molecules.

V. POSITIONS OF ANTIBONDING RESONANCES OF HOMONUCLEAR DIATOMIC MOLECULES

A remarkable feature of our analytical expressions (33)–(39) for the scattering-path operators τ is that they are functions of just the set of atomic phase shifts (or atomic t-matrix elements) and the dimensionless parameter $x(=k\rho)$, where ρ is the internuclear separation. For a homonuclear molecule, since $t=t^0$, the quantities τ depend only on a single set of t-matrix elements, t_l. Also, according to Eq. (12),

$$\mathrm{Re}t_l=\sin^2\delta_l, \quad \mathrm{Im}t_l=-\tfrac{1}{2}\cos 2\delta_l \tag{43}$$

so that, actually, only $\mathrm{Re}t_l$ is significant, because the imaginary part of t_l is determined by the real part:

$$\mathrm{Im}t_l=\pm\sqrt{-\mathrm{Re}t_l(1+\mathrm{Re}t_l)}, \tag{44}$$

Thus, using criterion (41), it is possible to plot a *universal curve* for the positions of resonances on a graph of x versus the real parts of the atomic t-matrix elements.

A. Universal curve for the π^* resonances

From the form (39) of the quantity Σ_π and criterion (41), it follows that the location of the π^* resonance depends only on the p-wave atomic scattering amplitude t_p. Thus, the *universal curve*, Fig. 4, for the positions of the π^* resonance consists of a plot for x versus $\mathrm{Re}(t_p)$. An interesting feature

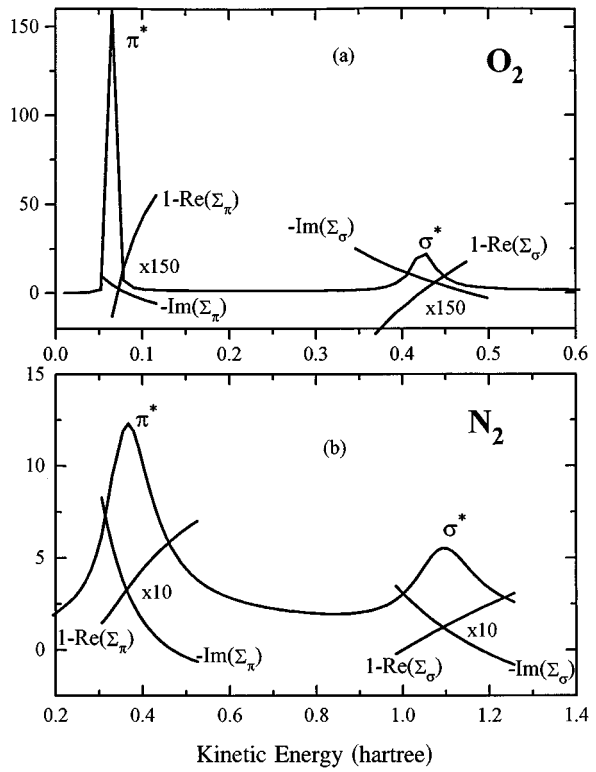

FIG. 3. Correspondence between the NEXAFS (arb. units) peak positions and the intersection points of the real and imaginary parts of the $1-\Sigma$ function for (a) oxygen and (b) nitrogen gas-phase molecules.

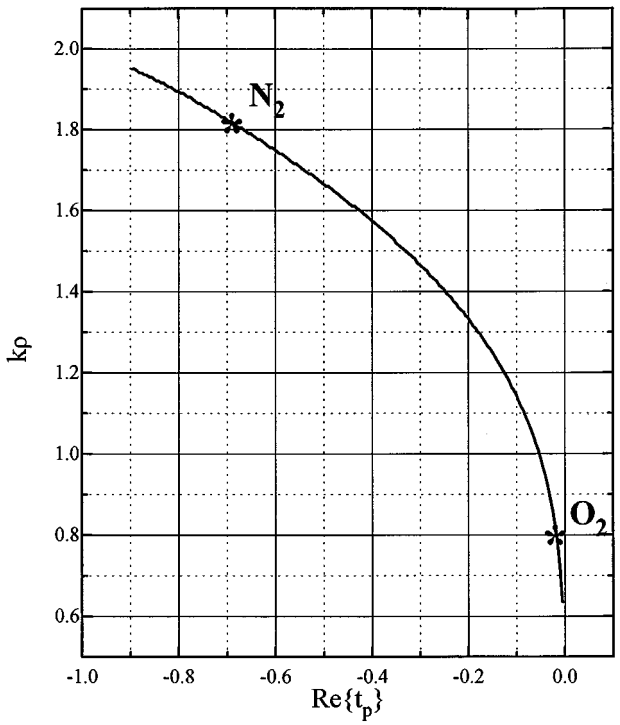

FIG. 4. Universal curve for the locations of π resonances. Dimensionless parameter $k\rho$ is equal to the product of electron wave number k and chemical bond length ρ. The abscissa indicates the values of the real part of the p-wave element of the atomic scattering amplitude t. The asterisks indicate the locations of the π resonances of the nitrogen and oxygen molecules.

of this curve is the absence of π^* resonances in the region corresponding to relatively high energies (or great internuclear separations), $x>2$.

Values, of atomic phase shifts and the mean potential between the atoms, may be calculated using the CCP-LDA method[12] mentioned earlier, or else a self-consistent muffin-tin calculation. For a homonuclear diatomic molecule, the value of $\mathrm{Re}(t_p)$ alone will allow one to read off a unique value of x from Fig. 4. From this, a determination may be made of the bond length of the molecule from a measured value of the resonance energy, or else the energy of the π^* resonance for a known bond length. The points on Fig. 4 corresponding to the π^* resonances of the O_2 and N_2 molecules are marked by asterisks.

B. A universal surface for the σ^* resonances

In the case of the σ^* resonances, the dimensionless quantity, x, is a function of the real parts of both t_s and t_p [as seen from Eq. (39)]. In this case, therefore, the universal curve of Fig. 4, must be replaced by a universal *surface*, as a function of both the s and p atomic scattering amplitudes.

VI. CONCLUSIONS

The theory of NEXAFS is much more complicated than that of EXAFS, due to the need to take account of the full multiple scattering of the ejected core electron in the former case. The key quantity that needs to be evaluated in NEXAFS is the so-called scattering-path operator τ, which represents the summation of all electron multiple-scattering paths beginning and ending on the atom absorbing the x-ray photon. As is usual in multiple-scattering calculations, the evaluation of τ usually requires the inversions of fairly large matrices, which are usually performed by computer.

In this paper we show that, at least in the case of diatomic molecules, the matrix inversions may be performed analytically to yield relatively simple explicit expressions for τ, and hence, for the x-ray-absorption rate, a measurable quantity. Excellent agreement is found between the results of our analytical expressions and standard computer simulations.

Our analytical expressions lead to the discovery of a *universal curve* for the π^* resonances of homonuclear diatomic molecules, relating a dimensionless quantity, x, the product of the ejected electron's wave number and the internuclear separation, to the real part of the p angular momentum component of the scattering amplitudes (or t matrices) of the constituent atoms. In the case of the σ^* resonances a *universal surface* is found, relating x to the real parts of both the s and p angular momentum components of the atomic t matrices.

The main previous analytical result for NEXAFS resonances is the so-called Natoli rule, which for diatomic molecules, suggests the simple relationship:

$$k\rho = \text{const}, \tag{45}$$

for the position of a resonance peak (in a scale of wave number k) and the bond length ρ. This was justified by the

multiple-scattering theories of Natoli,[15] and Rehr.[7] It is easy to see that our theory is consistent with this rule through the condition (41), which may be written $g(x)=0$, where g is some function. Thus, a resonance condition is maintained for variations of k and ρ, which keep $x=k\rho=$const. The expressions (39) for the Σ functions found in this paper allow the analytical evaluation of this constant.

ACKNOWLEDGMENTS

W.T.T. acknowledges support for this work from Department of Energy, Division of Chemical Sciences, Office of Basic Energy Sciences under Grant No. FG02-92ER14289, and D.K.S. is grateful for a research grant from the Petroleum Research Fund, administered by the American Chemical Society.

APPENDIX A

In calculating the matrix elements $\tau_{22}=\tau_{44}$ and τ_{33}, corresponding to the π^* and σ^* molecular orbitals (resonances), respectively, we take into consideration d-partial spherical harmonic, as well as s and p waves. For the sake of simplicity, we completely ignore g and f harmonics, since their contribution in the NEXAFS kinetic-energy range is negligibly small.

$$\begin{pmatrix}
1-R_{11}t_s^0 & 0 & -R_{13}t_p^0 & 0 & 0 & 0 & -R_{17}t_d^0 & 0 & 0 \\
0 & 1-R_{22}t_p^0 & 0 & 0 & 0 & -R_{26}t_d^0 & 0 & 0 & 0 \\
-R_{13}t_s^0 & 0 & 1-R_{33}t_p^0 & 0 & 0 & 0 & -R_{37}t_d^0 & 0 & 0 \\
0 & 0 & 0 & 1-R_{44}t_p^0 & 0 & 0 & 0 & -R_{48}t_d & 0 \\
0 & 0 & 0 & 0 & 1-R_{55}t_d^0 & 0 & 0 & 0 & 0 \\
0 & -R_{26}t_p^0 & 0 & 0 & 0 & 1-R_{66}t_d^0 & 0 & 0 & 0 \\
-R_{17}t_s^0 & 0 & -R_{37}t_p^0 & 0 & 0 & 0 & 1-R_{77}t_d^0 & 0 & 0 \\
0 & 0 & 0 & -R_{48}t_p^0 & 0 & 0 & 0 & 1-R_{88}t_d & 0 \\
0 & 0 & 0 & 0 & 0 & 0 & 0 & 0 & 1-R_{99}t_d^0
\end{pmatrix}$$

$$\times\begin{pmatrix}
. & x_{12} & x_{13} & . \\
. & x_{22} & x_{23} & . \\
. & x_{32} & x_{33} & . \\
. & x_{42} & x_{43} & . \\
. & x_{52} & x_{53} & . \\
. & x_{62} & x_{63} & . \\
. & x_{72} & x_{73} & . \\
. & x_{82} & x_{83} & . \\
. & x_{92} & x_{93} & .
\end{pmatrix}=\begin{pmatrix}
. & 0 & 0 & . \\
. & 1 & 0 & . \\
. & 0 & 1 & . \\
. & 0 & 0 & . \\
. & 0 & 0 & . \\
. & 0 & 0 & . \\
. & 0 & 0 & . \\
. & 0 & 0 & . \\
. & 0 & 0 & .
\end{pmatrix}.$$

Therefore, the set of coupled equations for determining

$$x_{22}=(1-Rt^0)^{-1}_{22}$$

is given by

$$\begin{pmatrix} 1-R_{22}t_p^0 & -R_{26}t_d^0 \\ -R_{26}t_p^0 & 1-R_{66}t_d^0 \end{pmatrix}\times\begin{pmatrix} x_{22} \\ x_{62} \end{pmatrix}=\begin{pmatrix} 1 \\ 0 \end{pmatrix}. \tag{A1}$$

The set of equations, which includes the matrix element

$$x_{33}=(1-Rt^0)^{-1}_{33}$$

is given by

$$\begin{pmatrix} 1-R_{11}t_s^0 & -R_{13}t_p^0 & -R_{17}t_d^0 \\ -R_{13}t_s^0 & 1-R_{33}t_p^0 & -R_{37}t_d^0 \\ -R_{17}t_s^0 & -R_{37}t_p^0 & 1-R_{77}t_d^0 \end{pmatrix}\times\begin{pmatrix} x_{13} \\ x_{33} \\ x_{73} \end{pmatrix}=\begin{pmatrix} 0 \\ 1 \\ 0 \end{pmatrix}. \tag{A2}$$

From Eq. (A1) it follows that

$$\tau_{22}=it_p^0x_{22}=\frac{it_p^0}{1-R_{22}t_p^0-\dfrac{(R_{26})^2t_p^0t_d^0}{1-R_{66}t_d^0}}. \tag{A3}$$

The solution of the Eq. (A2) is

$$x_{33}=\frac{\det\begin{pmatrix}1-R_{11}t_s^0 & 0 & -R_{17}t_d^0\\ -R_{13}t_s^0 & 1 & -R_{37}t_d^0\\ -R_{17}t_s^0 & 0 & 1-R_{77}t_d^0\end{pmatrix}}{\det\begin{pmatrix}1-R_{11}t_s^0 & -R_{13}t_p^0 & -R_{17}t_d^0\\ -R_{13}t_s^0 & 1-R_{33}t_p^0 & -R_{37}t_d^0\\ -R_{17}t_s^0 & -R_{37}t_p^0 & 1-R_{77}t_d^0\end{pmatrix}}, \tag{A4}$$

and may be rewritten as

$$\tau_{33}=it_p^0x_{33}=it_p^0[(1-R_{11}t_s^0)(1-R_{77}t_d^0)-(R_{17})^2t_s^0t_d^0]\times\{(1-R_{33}t_s^0)[(1-R_{11}t_s^0)(1-R_{77}t_d^0)-(R_{17})^2t_s^0t_d^0]$$
$$-2R_{13}R_{37}R_{17}t_s^0t_p^0t_d^0-(1-R_{77}t_d^0)(R_{13})^2t_s^0t_p^0-(1-R_{11}t_s^0)(R_{37})^2t_p^0t_d^0\}^{-1}. \tag{A5}$$

From Eq. (A3) and Eq. (A5), it follows that the expressions for both Σ_π and Σ_σ functions [which are determined by Eq. (38)] are

$$\Sigma_\pi=R_{22}t_p^0+\frac{(R_{26})^2t_p^0t_d^0}{1-R_{66}t_s^0},$$

$$\Sigma_\sigma=R_{33}t_s^0+\frac{2R_{13}R_{37}R_{17}t_s^0t_p^0t_d^0+(1-R_{77}t_d^0)(R_{33})^2t_s^0t_p^0+(1-R_{11}t_s^0)(R_{37})^2t_p^0t_d^0}{(1-R_{11}t_s^0)(1-R_{77}t_d^0)-(R_{17})^2t_s^0t_d^0}. \tag{A6}$$

APPENDIX B

In considering the analytical representation for the reflection matrix components $R_{lm,l'm'}\equiv R_{N,N'}$ [where $N=l(l+1)+m+1$] through Eq. (17), an explicit analytical form of the reexpansion coefficients (propagators) g^{oi} and g^{io} is required. For diatomic molecules ($i=1$), only two matrices should be determined: $g^{oi}\equiv g(+)$ and $g^{oi}\equiv g(-)$.

The $g(+)$ matrix describes the electron moving from the central atom to its neighbor and is given by Eq. (26):

$$g_{lm,l'm}(+)=\sqrt{4\pi}\sum_{l''}\sqrt{2l''+1}(-1)^m i^{l-l'-l''}h_{l''}^{(l)}(k\rho)B(lm,l'm,l''0), \tag{B1}$$

where ρ is the internuclear separation.

For the reverse motion after backscattering, the expression (B1) is still valid with the additional factor $(-1)^{l''}$, due to the spherical harmonic transformation under inversion in Eq. (23),

$$g_{lm,l'm}(-)=\sqrt{4\pi}\sum_{l''}(-1)^{l''}\sqrt{2l''+1}(-1)^m i^{l-l'-l''}h_{l''}^{(1)}(k\rho)B(lm,l'm,l''0). \tag{B2}$$

Some of the reflection matrix components required for the calculation of x-ray absorption, for diatomic molecules, are given below. Note that they are calculated including harmonics up to $l=2$. The argument is $x=k\rho$.

$$R_{11,11}\equiv R_{44}=\left(\frac{3h_1^{(1)}(x)}{x}\right)^2t_p+3\left(\frac{5h_2^{(1)}(x)}{x}\right)^2t_d, \tag{B3}$$

$$R_{10,10}\equiv R_{33}=(\sqrt{3}h_1^{(1)}(x))^2t_s+[h_0^{(1)}(x)-2h_2^{(1)}(x)]^2t_p+\tfrac{3}{5}[2h_1^{(1)}(x)-3h_3^{(1)}(x)]^2t_d, \tag{B4}$$

$$R_{00,10}\equiv R_{13}=\sqrt{3}h_0^{(1)}(x)h_1^{(1)}(x)t_s-\sqrt{3}[h_0^{(1)}(x)-2h_2^{(1)}(x)]h_1^{(1)}(x)t_p-\sqrt{3}[2h_1^{(1)}(x)-3h_3^{(1)}(x)]h_2^{(1)}(x)t_d, \tag{B5}$$

$$R_{00,00}\equiv R_{11}=(h_0^{(1)}(x))^2t_s+3(h_1^{(1)}(x))^2t_p+5(h_2^{(1)}(x))^2t_d, \tag{B6}$$

$$R_{11,21}\equiv R_{48}=R_{26}=\frac{9\sqrt{5}}{x^2}h_1^{(1)}(x)h_2^{(1)}(x)t_p+\frac{3\sqrt{5}}{x}h_2^{(1)}(x)[h_0^{(1)}(x)-\tfrac{5}{7}h_2^{(1)}(x)-\tfrac{12}{7}h_4^{(1)}(x)]t_d, \tag{B7}$$

$$R_{21,21}\equiv R_{88}=R_{66}=\left(\frac{3\sqrt{5}}{x}h_2^{(1)}(x)\right)^2t_p+[h_0^{(1)}(x)-\tfrac{5}{7}h_2^{(1)}(x)-\tfrac{12}{7}h_4^{(1)}(x)]^2t_d, \tag{B8}$$

$$R_{00,20}\equiv R_{17}=\sqrt{5}h_0^{(1)}(x)h_2^{(1)}(x)t_s-\frac{3}{\sqrt{5}}h_1^{(1)}(x)[2h_1^{(1)}(x)-3h_3^{(1)}(x)]t_p+\sqrt{5}h_2^{(1)}(x)[h_0^{(1)}(x)-\tfrac{10}{7}h_2^{(1)}(x)+\tfrac{18}{7}h_4^{(1)}(x)]t_d\,, \tag{B9}$$

$$R_{10,20}\equiv R_{37}=\sqrt{15}h_1^{(1)}(x)h_2^{(1)}(x)t_s-\sqrt{\tfrac{3}{5}}[h_0^{(1)}(x)-2h_2^{(1)}(x)][2h_1^{(1)}(x)-3h_3^{(1)}(x)]t_p-\sqrt{\tfrac{3}{5}}[2h_1^{(1)}(x)-3h_3^{(1)}i(x)][h_0^{(1)}(x)$$
$$-\tfrac{10}{7}h_2^{(1)}(x)+\tfrac{18}{7}h_4^{(1)}(x)]t_d\,, \tag{B10}$$

$$R_{20,20}\equiv R_{77}=(\sqrt{5}h_2^{(1)}(x))^2t_s+\tfrac{3}{5}[2h_1^{(1)}(x)-3h_3^{(1)}(x)]^2t_p+[h_0^{(1)}(x)-\tfrac{10}{7}h_2^{(1)}(x)+\tfrac{18}{7}h_4^{(1)}(x)]t_d\,. \tag{B11}$$

[1] E.A. Stern, D.E. Sayers, and F.W. Lytle, Phys. Rev. B **11**, 4836 (1975).

[2] C.A. Ashley and S. Doniach, Phys. Rev. B **11**, 1279 (1975).

[3] P.A. Lee and J.B. Pendry, Phys. Rev. B **11**, 2795 (1975).

[4] P.J. Durham, J.B. Pendry, and C.H. Hodges, Comput. Phys. Commun. **25**, 193 (1982).

[5] D.D. Vvedensky, D.K. Saldin, and J.B. Pendry, Comput. Phys. Commun. **4**, 421 (1986).

[6] T.A. Tyson, K.O. Hodgson, C.R. Natoli, and M. Benfatto, Phys. Rev. B **46**, 5997 (1992).

[7] J.J. Rehr, R.C. Albers, and S.I. Zabinski, Phys. Rev. Lett. **69**, 3397 (1992).

[8] J. Stohr, *NEXAFS Spectroscopy* (Springer, Heidelberg, 1992).

[9] H.Bethe and E.E. Saltpeter, *Quantum Mechanics of One and Two-Electron Atoms* (Plenum, New York, 1977).

[10] J.S. Faulkner and G.M. Stocks, Phys. Rev. B **21**, 3222 (1980).

[11] J.B. Pendry, *Low Energy Electron Diffraction* (Academic, London, 1974).

[12] V.L. Shneerson, W.T. Tysoe, and D.K. Saldin, Phys. Rev. B **51**, 13 015 (1995).

[13] V.L. Shneerson, D.K. Saldin, and W.T. Tysoe, Surf. Sci. (to be published).

[14] A. Bianconi, H. Petersen, F.C. Brown, and R.Z. Bachrach, Phys. Rev. A **17**, 1907 (1978).

[15] C.R. Natoli, in *EXAFS and Near Edge Structure III*, edited by K.O. Hodgson, B. Hedman, and J.E. Penner-Hahn (Springer-Verlag, Berlin, 1984), p. 38.